

Assessment of radiative feedback in climate models using satellite observations of annual flux variation

Yoko Tsushima^{a,1} and Syukuro Manabe^b

^aMet Office Hadley Centre, Exeter EX1 3PB, United Kingdom; and ^bProgram in Atmospheric and Oceanic Sciences, Princeton University, Princeton, NJ 08544

Edited* by V. Ramanathan, University of California at San Diego, La Jolla, CA, and approved March 20, 2013 (received for review December 3, 2012)

In the climate system, two types of radiative feedback are in operation. The feedback of the first kind involves the radiative damping of the vertically uniform temperature perturbation of the troposphere and Earth's surface that approximately follows the Stefan-Boltzmann law of blackbody radiation. The second kind involves the change in the vertical lapse rate of temperature, water vapor, and clouds in the troposphere and albedo of the Earth's surface. Using satellite observations of the annual variation of the outgoing flux of longwave radiation and that of reflected solar radiation at the top of the atmosphere, this study estimates the so-called "gain factor," which characterizes the strength of radiative feedback of the second kind that operates on the annually varying, global-scale perturbation of temperature at the Earth's surface. The gain factor is computed not only for all sky but also for clear sky. The gain factor of so-called "cloud radiative forcing" is then computed as the difference between the two. The gain factors thus obtained are compared with those obtained from 35 models that were used for the fourth and fifth Intergovernmental Panel on Climate Change assessment. Here, we show that the gain factors obtained from satellite observations of cloud radiative forcing are effective for identifying systematic biases of the feedback processes that control the sensitivity of simulated climate, providing useful information for validating and improving a climate model.

CERES | cloud feedback | CMIP | metric of radiative feedback | ERBE

One of the most challenging tasks of climate science is to determine climate sensitivity. It is often defined as the equilibrium response of the global mean surface temperature to the doubling of atmospheric CO₂. Unfortunately, currently available models have sensitivities that vary across a wide range. According to the report of the fourth Intergovernmental Panel on Climate Change (IPCC) assessment (1), about two-thirds of the current climate models have sensitivities that range between 2 °C and 4.5 °C. Although this range is itself large, the sensitivities of one-third of the models lie outside of this range. The need to reduce this sizable uncertainty is one of the important reasons it is urgent to understand and reliably quantify the mechanisms that determine climate sensitivity.

Climate sensitivity is inversely proportional to the strength of the radiative feedback that operates on the global-scale perturbation of surface temperature. Here, we describe our attempt to estimate the strength of the radiative feedback that operates on the global-scale perturbation of surface temperature in many current climate models and compare the results with those obtained from satellite observations. The geographical pattern of the perturbation chosen for the present analysis, however, is the annual variation, rather than global warming.

The annual variation of the global mean surface temperature is attributable mainly to the difference in the amplitude of the seasonal variation of the hemispheric mean temperature that is out of phase between the two hemispheres. Because the amplitude of the seasonal variation is much larger over continents than over oceans, the seasonal variation of hemispheric mean surface temperature is substantially larger over the Northern Hemisphere than over the Southern Hemisphere, which is mostly covered by ocean. This is the main reason why the annual variation of the global surface temperature is in phase with that of the Northern Hemisphere.

The annual range of the global mean surface temperature is about 3 K, with the highest temperature in July and the lowest in January. The range is comparable in magnitude to the current estimate of the equilibrium response of the global mean surface temperature to the doubling of CO₂ concentration in the atmosphere (2). Although the geographical pattern of the annual variation is quite different from that of global warming simulated by the model, the annual variation of the global mean surface temperature yields the annual range of the top-of-the-atmosphere (TOA) flux of outgoing radiation that is large enough to be detectable using satellite observations. One can argue whether the strength of the feedback inferred from the annual variation is relevant to global warming. Nevertheless, it can provide a powerful constraint against which every climate model should be validated.

The first attempt to estimate the strength of the radiative feedback on the annual variation was made by Inamdar and Ramanathan (3). Using the TOA flux of outgoing longwave radiation (OLR) obtained from the Earth Radiation Budget Experiment (ERBE) (4), they estimated the strength of the clear-sky feedback that operates on the annual variation of the global mean surface temperature. The strength thus obtained turned out to be similar to the strength of the clear-sky feedback obtained from the CO₂-doubling experiments that were conducted using 3D models (5). The agreement suggests that the strength of the longwave feedback does not depend much upon the geographical distribution of surface temperature.

The study (3) was followed by that of Tsushima and Manabe (6). Using the TOA fluxes of OLR and reflected solar radiation obtained from ERBE, they estimated the gain factor of the annual variation not only for clear sky but also for all sky. From the difference between the two gain factors thus obtained, they estimated the gain factor of cloud radiative forcing (CRF), which represents the overall contribution of cloud to radiative feedback (the definition of CRF is given in *Methods, Gain Factors*), and found that the gain factors of both longwave and solar CRF are small. The gain factors thus obtained were compared with those from three general circulation models.

The present study is the natural extension of the studies of Tsushima and Manabe (6) and Tsushima et al. (7), which evaluates the strength of the radiative feedback using the TOA fluxes obtained from satellite observation and compares it with that obtained from climate models. Since the publication of refs. 6 and 7, the annual variation of TOA fluxes has become available from the 35 models that have been used for the fourth and the fifth IPCC assessments. Meanwhile, new datasets from Clouds and the Earth's Radiant Energy System (CERES) satellite observations (8, 9) with improved accuracy have also become available, motivating us to conduct the present study.

Results and Discussion

As noted in *Methods, Gain Factors*, the so-called "feedback parameter" (λ) represents the strength of the radiative feedback that operates on the perturbation of the global mean surface temperature. It may be subdivided into the feedback of the first kind (λ_0)

Author contributions: Y.T. and S.M. designed research; Y.T. performed research; Y.T. analyzed data; and S.M. wrote the paper.

The authors declare no conflict of interest.

*This Direct Submission article had a prearranged editor.

¹To whom correspondence should be addressed. E-mail: yoko.tsushima@metoffice.gov.uk.

and that of the second kind (λ_F) as expressed by $\lambda = \lambda_0 + \lambda_F$. Here, the feedback of the first kind represents the radiative damping of the vertically uniform temperature perturbation of the troposphere and the Earth's surface that follows approximately the Stefan-Boltzmann law of blackbody radiation. The feedback of the second kind involves the changes in the vertical lapse rate of temperature, absolute humidity, and clouds in the troposphere and albedo at the Earth's surface. To characterize the strength of the radiative feedback of the second kind, a nondimensional metric "gain factor" (g), introduced by Hansen et al. (10), is used here. It is defined as $g = -\lambda_F/\lambda_0$, where the sign of the gain factor is chosen such that it is positive when a positive feedback is in operation, enhancing the sensitivity of climate. However, the reverse is the case if the gain factor is negative. If the gain factor is positive and is close to 1, for example, the feedback of the second kind almost cancels that of the first kind. In this case, the feedback parameter is small and the sensitivity is large. In short, the gain factor indicates the degree by which the feedback of the second kind counteracts that of the first kind and weakens the overall strength of radiative feedback, thereby enhancing the sensitivity of climate.

In the present study, three sets of satellite observation (*Methods, Data from Observations*) are used for the computation of the gain factors of the radiative feedback that operates on the annual variation. They are ERBE (4) and two versions [Monthly TOA/Surface Averages (SRBAVG) and Energy Balanced and Filled (EBAF)] of CERES (8, 9). Here we present the result from CERES SRBAVG as an example.

To estimate the gain factor of the longwave feedback of the annual variation as described in *Methods, Computational Procedure*, the globally averaged, monthly mean TOA fluxes of the OLR from CERES SRBAVG are plotted against those of the global mean surface temperature for the 12 mo of a year (Fig. 1*A*). The slope of the regression line through the scatter plots represents the longwave component of the feedback parameter. It is smaller than the slope of the dashed line that indicates the strength of the feedback of the first kind. From the difference between the two slopes, one can estimate the gain factor of the longwave feedback of the second kind that operates on the annual variation. The feedback analysis is also performed for clear sky as shown in Fig. 1*B*.

Inspecting Fig. 1*A* and *B*, one notes that the slope of the regression line through the scatter plots is quite similar between the two, indicating that the strength of radiative feedback is similar between the all sky and clear sky. This explains why the regression line is almost horizontal in Fig. 1*C*, indicating that the longwave CRF hardly depends upon the surface temperature at the global scale. The gain factor of the longwave feedback for all sky obtained here is 0.28 and is similar to 0.32 (i.e., that of clear-sky feedback), yielding -0.04 as the gain factor of longwave CRF. The result presented here suggests that clouds have relatively small effect upon the longwave feedback that operates on the annual variation. This is in agreement with the results obtained from the other two sets of data obtained from satellite observation used here.

Similar feedback analysis is performed for the solar feedback that operates on the annual variation as described in *Methods, Computational Procedure*. Fig. 2*A* and *B* illustrates, for all sky and clear sky, the scatter plots between the monthly mean value of global mean TOA flux of annually normalized, reflected solar radiation (defined in *Methods, Gain Factors*) and that of the global mean surface temperature. In Fig. 2*A* and *B*, the TOA flux decreases with increasing surface temperature. The figures also reveal that the rate of reduction decreases with increasing temperature, probably owing to the dependence of the snow albedo feedback upon temperature. It is notable, however, that the slope of the regression line through the scatter plots is similar between all sky and clear sky, suggesting that the strength of solar feedback may be similar between the two. This explains why the regression line is almost horizontal in Fig. 2*C*, indicating that solar CRF depends little upon surface temperature on the global scale. From the slope of the regression line through the scatter plots, one can compute the solar gain factors, which are 0.39 for all sky, 0.32 for clear sky, and 0.07 for solar CRF. The results presented here suggest that the overall contribution of clouds to solar feedback may be relatively small, in agreement with the result obtained earlier from ERBE (6). It does not agree,

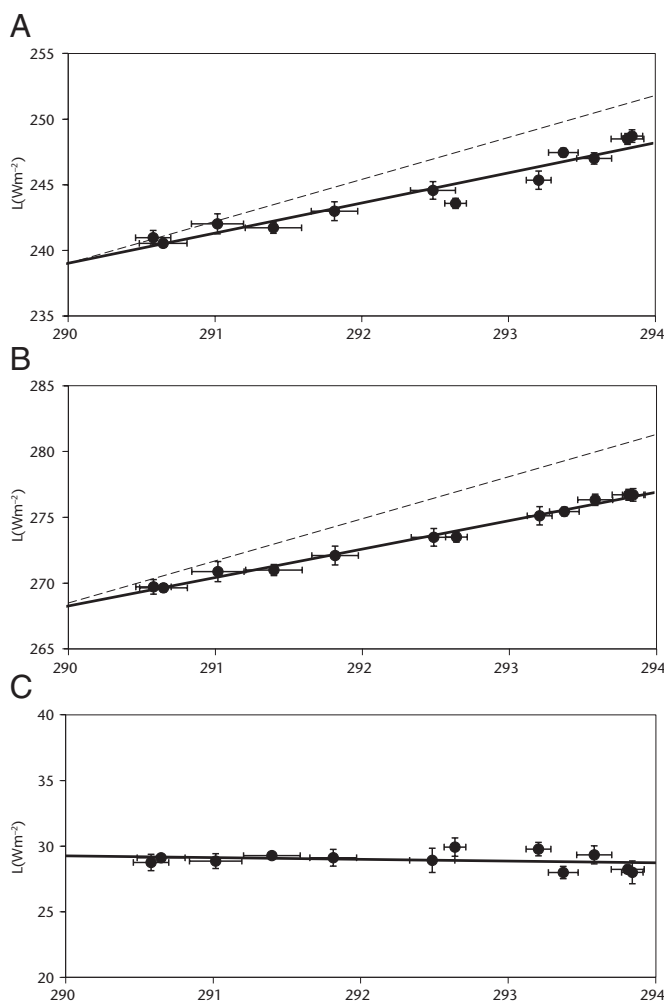


Fig. 1. The globally averaged, monthly mean TOA flux of outgoing longwave radiation (Wm^{-2}) over all sky (*A*) and clear sky (*B*) and the difference between them (i.e., longwave CRF) (*C*) are plotted against the global mean surface temperature (K) on the abscissa. The vertical and horizontal error bar on the plots indicates SD. The solid line through scatter plots is the regression line. The slope of dashed line indicates the strength of the feedback of the first kind (λ_0).

however, with the result from CERES EBAF, as described later in this section.

Adding longwave and solar gain factors, one can determine the total gain factor of the all-sky feedback that operates on the annual variation. It is 0.67 and is slightly larger than 0.64 (i.e., the gain factor of the clear-sky feedback). From the difference between the two gain factors, one can determine the total gain factor of CRF. It is 0.03 and is very small. This result suggests that the overall contribution of clouds to radiative feedback on the annual variation may be relatively small, in agreement with the result obtained earlier from ERBE (6).

The total gain factor of the annual variation obtained here (i.e., 0.67) can be compared with that of global warming obtained from climate models. Soden and Held (11) estimated the total gain factors of the models used for the fourth IPCC assessment and obtained 0.59 ± 0.12 . This implies that the average sensitivity (i.e., the equilibrium response to CO_2 doubling) of the models is $\sim 2.9^\circ\text{C}$. Coleman (12) estimated the average gain factor of the set of the models developed earlier and obtained 0.67 ± 0.12 with an implied sensitivity of $\sim 3.6^\circ\text{C}$. In short, the total gain factor of the annual variation obtained from satellite observations is comparable in magnitude to those of global warming.

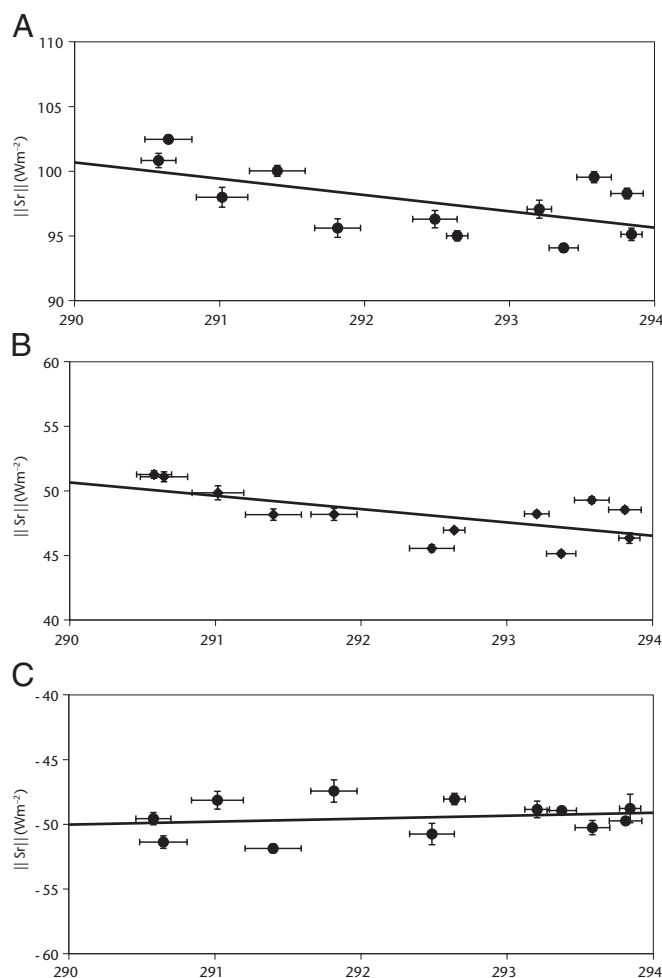


Fig. 2. The globally averaged, monthly mean TOA flux (Wm^{-2}) of annually normalized, reflected solar radiation over all sky (A) and clear sky (B) and the difference between them (C) (i.e., solar CRF) are plotted against the global mean surface temperature (K) on the abscissa. The vertical and horizontal error bar on the plots indicates SD. The solid line through scatter plots is the regression line.

Using the outputs from the 18 Coupled Model Intercomparison Project (CMIP) 3 and 17 CMIP5 models (*Methods, Data from Models*) used for the fourth and fifth IPCC assessments, respectively, the gain factors of the longwave, solar, and total feedback of the annual variation were estimated for both all sky and clear sky. The longwave, solar, and total gain factors of CRF are then computed as the difference between the gain factors of all sky and those of clear sky. The gain factors thus obtained are compared with those obtained using the three sets of satellite observations identified above.

The average gain factor of the longwave clear-sky feedback obtained from the CMIP models is 0.43 and is larger than 0.42, 0.32, and 0.36 (i.e., the gain factors obtained from ERBE, CERES SRBAVG, and CERES EBAF, respectively). Nevertheless, they are in fairly good agreement with those obtained from satellite observation, as shown in Fig. 3B, confirming the result obtained earlier by Inamdar and Ramanathan (3). The agreement is not as good with regard to the longwave gain factor of the all sky, which has larger intermodel variation (Fig. 1A), owing mainly to the discrepancy in the longwave gain factors of CRF described below. The average value of the CMIP models is 0.52 and is substantially larger than the 0.35, 0.28, and 0.31 obtained from the three satellite observations identified above.

With regard to the longwave gain factors of CRF shown in Fig. 3C, all gain factors obtained from satellite observations have small negative values, as shown on the left-hand side of the figure, in

agreement with the results obtained by Tsushima and Manabe (6). Although two models have large positive values and a few models have negative values, most (30 out of 35) of the CMIP models have positive values, with an average of 0.08 ± 0.04 , and are opposite in sign from the -0.07 , -0.04 , and -0.05 obtained from the three satellite observations. In short, the gain factors of longwave CRF obtained from most of the CMIP models have positive values, in contrast to the small negative values obtained from satellite observations. The former is larger than the latter by about 0.13.

A similar comparison is also made of the solar gain factors of clear-sky feedback. As Fig. 4B shows, the gain factors obtained from the CMIP models are in general agreement with those obtained from satellite observation. The spread among the gain factors, however, is much larger than the spread among the gain factors of the longwave clear-sky feedback shown in Fig. 3B. The average gain factor of the solar clear-sky feedback of the CMIP models is 0.30 and is similar to the 0.32 obtained from both ERBE and CERES SRBAVG but is larger than the 0.18 obtained from CERES EBAF. Due in no small part to the strong albedo feedback that involves large seasonal excursion of snow over continents, it is almost twice as large as the gain factor of the solar clear-sky feedback that operates on global warming in a typical climate model.

As Fig. 4C shows, there is a huge spread among the gain factors of solar CRF obtained from the CMIP models. Upon close inspection, one finds that it is possible to subdivide the 35 models into two groups. The 10 models in the first group have large negative gain factors, whereas the 25 models of the second group have gain factors that are much smaller. The average gain factor of solar CRF obtained from the first group of 10 models is -0.4 ± 0.1 , which is quite different from the positive gain factors obtained from satellite observations. However, the average gain factor of the remaining 25 models is 0.0 ± 0.1 . It is not significantly different from 0.04 and 0.07 (i.e., the gain factors obtained from ERBE and CERES SRBAVG, respectively), but it is substantially smaller than 0.23 (the estimate from CERES EBAF). Although CERES EBAF was constructed more recently than CERES SRBAVG, further analysis may be necessary to determine which gain factor is more realistic. Because of the difference between the two versions of CERES, the gain factor of the solar CRF is not as useful in identifying the systematic bias of the model as that of longwave CRF. Nevertheless, the gain factors of solar CRF from the majority (i.e., the second group) of the CMIP models is much closer to those obtained from satellite observations than to those from the minority (first) group, suggesting that the majority is likely to be more realistic than the minority.

The total gain factors of clear-sky feedback obtained from the CMIP models are compared with satellite observations in Fig. 5B. In general, the former is comparable in magnitude to the latter. The average total gain factor of clear-sky feedback of the CMIP model is 0.73 and is similar in magnitude to the 0.74 and 0.64 obtained from ERBE and CERES SRBAVG, respectively. It is, however, substantially larger than the 0.54 obtained from CERES EBAF. The difference in total gain factors between the two versions of CERES is attributable mainly to the difference in the solar gain factor of clear sky mentioned above (Fig. 4B).

The average total gain factor of all sky feedback of the CMIP models is 0.71. It is similar in magnitude to the 0.71, 0.67, and 0.73 obtained from ERBE, CERES SRBAVG, and CERES EBAF, respectively. One should note, however, that the total gain factor varies greatly among the CMIP models, as shown in Fig. 5A, due in no small part to the intermodel difference in the gain factor of CRF shown in Fig. 5C.

As discussed above, the gain factors of radiative feedback of the annual variation are useful for detecting systematic biases of the modeled feedback, providing information that is very useful for improving climate models. This is particularly so with regard to the gain factor of CRF that varies greatly among the current climate models.

It is well recognized that parameterization of cloud processes is one of the most difficult problems in climate modeling. Unfortunately, it has been very difficult, if not impossible, to determine large numbers of parameters of cloud microphysical processes

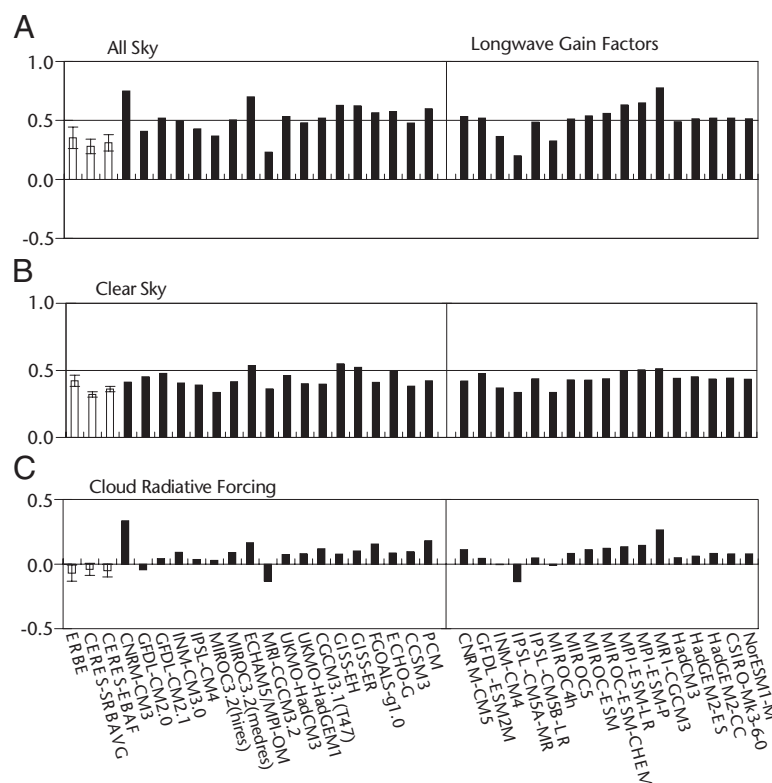


Fig. 3. The gain factors of longwave feedback that operates on the annual variation of the global mean surface temperature. (A) All sky. (B) Clear sky. (C) Cloud radiative forcing. Blank bars on the left indicate the gain factors obtained from satellite observation (ERBE, CERES SRBVG, and CERES EBAF) with the SE bar. Black bars indicate the gain factors obtained from the models identified by acronyms at the bottom of the figure (*Methods, Data from Models*). The vertical line near the middle of each frame separates the CMIP3 models on the left from the CMIP5 models on the right.

individually based upon observations. It is therefore desirable to constrain macroscopically the parameterization of cloud processes as a whole, using large-scale observation from satellites. Although the gain factors of CRF differ from those of the cloud feedback, as

explained in *Methods*, *Gain Factors*, they may be computed directly from the regression analysis between global TOA fluxes and global mean surface temperature and are ideally suited to this purpose.

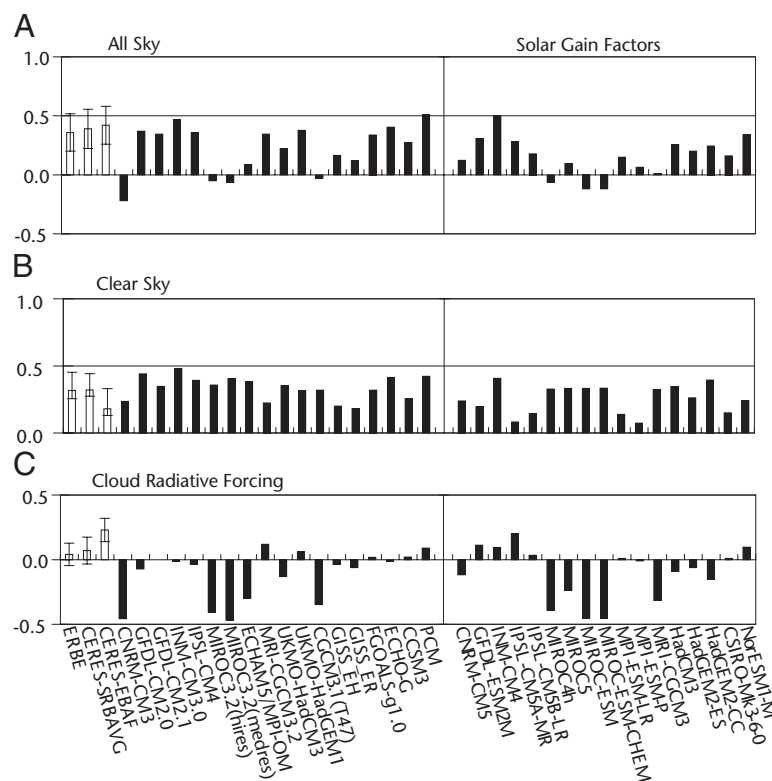


Fig. 4. The gain factors of solar feedback that operate on the annual variation of the global mean surface temperature. (A) All sky. (B) Clear sky. (C) Cloud radiative forcing. See Fig. 3 legend for further explanation.

sensitivity of climate, if gain factor is positive. However, the reverse is the case if the gain factor is negative. Using the gain factor thus defined, the feedback parameter (λ) can be expressed as

$$\lambda = \lambda_0(1 - g). \quad [7]$$

The gain factor (g) is subdivided into longwave and solar components as given by

$$g = g_L + g_S, \quad [8]$$

where g_L and g_S are given by

$$g_L = -\frac{1}{\lambda_0}(\lambda_L - \lambda_0) \quad [9]$$

$$g_S = -\frac{1}{\lambda_0}\lambda_S, \quad [10]$$

where $\lambda_L = \frac{d[\lambda]}{dT_s}$ and $\lambda_S = \frac{d[\lambda_S]}{dT_s}$.

The term “cloud radiative forcing” was introduced by Charlock and Ramanathan (16) to represent the effect of clouds upon the radiative heat budget of the Earth. The gain factor of cloud radiative forcing may be expressed as the difference between the gain factor of all sky and that of clear sky by

$$g_{CF} = g - g^{clear\ sky}. \quad [11]$$

The gain factor of cloud radiative forcing represents the total contribution of clouds to radiative feedback as a whole. As noted by Soden et al. (17), it is the sum of the gain factor of cloud feedback and that of the cloud masking or noncloud feedback.

Computational Procedure. To estimate the longwave component of the feedback parameter of the annual variation, the monthly mean values of the global mean TOA flux of OLR are plotted against those of the global mean surface temperature for the 12 mo of a year. From the slope of the regression line through the scatter plots, we estimated the longwave component of the feedback parameter, from which we computed the longwave gain factor, using Eq. 9.

To estimate the gain factor of the solar feedback, similar regression analysis is conducted. The monthly mean values of the global mean TOA fluxes of the annually normalized, reflected solar radiation are plotted against those of the global mean surface temperature for the 12 mo of a year. From the slope of the regression line through the scatter plots, we estimated the solar component of the feedback parameter, from which we computed the solar gain factor, using Eq. 10.

Because solar radiation is absent in the polar region during polar night, it is not possible to obtain the annually normalized, reflected solar radiation. This is the main reason why the global mean values of TOA fluxes of radiation and those of surface temperature are averaged over the area between 60°N and 60°S rather than over the entire globe for the regression analysis conducted here. For the sake of comparison, the identical averaging procedure is used for the analysis of model data. In short, the term “global mean” indicates the averaging over the area between 60°N and 60°S rather than over the entire globe.

Data from Observations. The TOA fluxes of longwave and reflected solar radiation used here are obtained from two sets of satellite observation. One is the ERBE conducted over the 5-y period from February 1985 to February 1990 (4). The other is the CERES, conducted over the 5.5-y period from March 2000 to October 2005 (8). Two versions of the CERES data analysis (8, 9) are used in this study. In the first version, CERES SRBAVG (SRBAVG1-Terra-FM1- MODIS-Edition2D-GEO) (8), the TOA fluxes are estimated from unfiltered radiances using new angular distribution models (18, 19). In the second version, called CERES EBAF (9), the global monthly mean TOA fluxes of the CERES SRBAVG are adjusted such that they are consistent with the observed, global heat storage of the Earth–atmosphere system. In addition, an attempt was made to improve the solar clear-sky feedback using high-resolution Moderate-Resolution Imaging Spectroradiometer (MODIS) measurements (20).

The data of surface temperature are obtained from the reanalysis of the daily weather data that was conducted jointly by the National Center for Environmental Prediction and National Center for Atmospheric Research (21) for the corresponding periods when CERES and ERBE were in operation, respectively.

To conduct the regression analysis described in the preceding section, the 12 monthly values of the global mean TOA flux of OLR and those of annually normalized reflected solar radiation are obtained and are averaged over the 5- and 5.5-y periods of ERBE and CERES, respectively. They are plotted against the 12 monthly values of surface temperature averaged over the same periods.

Data from Models. We use outputs from 18 and 17 models that participated in the CMIP3 (22) and CMIP5 (23) as parts of the fourth and fifth IPCC assessments, respectively. In total, 35 CMIP models are used. For the names of institutions that constructed the CMIP3 and CMIP5 models, see www-pcmdi.llnl.gov/ipcc/about_ipcc.php and <http://cmip-pcmdi.llnl.gov/cmip5/citation.html>, respectively. The variables used in this study are surface air temperature, the TOA flux of OLR, reflected solar radiation for both all sky and clear sky, with clouds artificially removed in the latter. It should be noted here that, for the analysis of the model feedback, surface air temperature is used instead of skin surface temperature, following the practice used in the previous studies. According to the test computation, the result of our feedback analysis is not very sensitive to the choice of observations identified above.

ACKNOWLEDGMENTS. We thank Drs. Alejandro Bodas-Salcedo, Jonathan Gregory, William Ingram, and Mark Ringer at the UK Met Office Hadley Centre, whose useful comments improved the manuscript. We also thank the Program for Climate Model Diagnosis and Intercomparison and World Climate Research Programme’s Working Group on Coupled Modeling for making available the multimodel dataset obtained from the Coupled Model Intercomparison Project supported by the Office of Science, US Department of Energy. This work was funded by European Union (EU) Seventh Framework Programme (FP7/2007–2013) Grant 244067 for the EU Cloud Intercomparison and Process Study Evaluation Project, Joint Department of Energy and Climate Change/Defra Met Office Hadley Centre Climate Programme Grant GA01101, and the Global Environment Research Fund (S-5) from the Ministry of the Environment (Japan).

- Meehl GA, et al. (2007) Global climate projections. *Climate Change 2007: The Physical Science Basis. Contribution of Working Group I to the Fourth Assessment Report of the Intergovernmental Panel on Climate Change*, ed Solomon S, et al. (Cambridge Univ Press, Cambridge, UK).
- Webb MJ, et al. (2006) On the contribution of local feedback mechanisms to the range of climate sensitivity in two GCM ensembles. *Clim Dyn* 27:17–38.
- Inamdar AK, Ramanathan V (1998) Tropical and global scale interaction among water vapor, atmospheric greenhouse effect and surface temperature. *J Geophys Res* 103: 32177–32194.
- Harrison EF, et al. (1990) Seasonal variation of cloud radiative forcing derived from the Earth Radiation Budget Experiment. *J Geophys Res* 95:18687–18703.
- Mitchell JFB (1989) The “greenhouse effect” and climate change. *Rev Geophys* 27:115–139.
- Tsushima Y, Manabe S (2001) Influence of cloud feedback on the annual variation of the global mean surface temperature. *J Geophys Res* 106:22635–22646.
- Tsushima Y, Abe-Ouchi A, Manabe S (2005) Radiative damping of annual variation in global mean surface temperature: Comparison between observed and simulated feedback. *Clim Dyn* 24:591–597.
- Wielicki BA, et al. (1996) Clouds and the Earth’s Radiant Energy System (CERES): An Earth observing system experiment. *Bull Am Meteorol Soc* 77:853–868.
- Loeb NG, et al. (2009) Toward optimal closure of the Earth’s top-of-atmosphere radiation budget. *J Clim* 22:748–766.
- Hansen J, et al. (1984) In Climate sensitivity: Analysis of feedback mechanisms. *Climate Processes and Climate Sensitivity*, eds Hansen J, Takahashi MH (Am Geophysical Union, Washington, DC), Vol 29, pp130–163.
- Soden BJ, Held IM (2006) An assessment of climate feedbacks in coupled ocean–atmosphere models. *J Clim* 19:3354–3360.
- Colman R (2003) A comparison of climate feedback in general circulation models. *Clim Dyn* 20:865–873.
- Wetherald RT, Manabe S (1988) Cloud feedback processes in a general circulation model. *J Atmos Sci* 45:1397–1415.
- Gregory JM, et al. (2004) A new method for diagnosing radiative forcing and climate sensitivity. *Geophys Res Lett* 31:L03205, 10.1029/2003GL018747.
- Cess RD, et al. (1997) Comparison of the seasonal change in cloud-radiative forcing from atmospheric general circulation models and satellite observations. *J Geophys Res* 102:16593–16603.
- Charlock T, Ramanathan V (1985) The albedo field and cloud radiative forcing in a general circulation model with internally generated cloud optics. *J Atmos Sci* 42:1408–1429.
- Soden BJ, Broccoli AJ, Hemler RS (2004) On the use of cloud forcing to estimate cloud feedback. *J Clim* 17:3661–3665.
- Loeb NG, et al. (2003) Angular distribution models for top-of-atmosphere radiative flux estimation from the Clouds and the Earth’s Radiant Energy System instrument on the tropical rainfall measuring mission satellite. Part I: Methodology. *J Appl Meteorol* 42:240–265.
- Loeb NG, Kato S, Lucachine K, Smith NM (2005) Angular distribution models for top-of-atmosphere radiative flux estimation from the Clouds and the Earth’s Radiant Energy System instrument on the Terra satellites. Part I: Methodology. *J Atmos Ocean Technol* 22:338–351.
- Minnis PG, et al. (2003) CERES cloud property retrievals from imagers on TRMM, Terra, and Aqua. *Remote Sensing of Clouds and the Atmosphere VIII*, eds Schaefter KP et al. (Int Soc Optics Photonics, Bellingham, WA), Vol 5235, pp 37–48.
- Kalnay E, et al. (1996) The NCEP/NCAR 40-year reanalysis project. *Bull Am Meteorol Soc* 77:437–471.
- Meehl GA, et al. (2007b) The WCRP CMIP3 multimodel dataset: A new era in climate change research. *Bull Am Meteorol Soc* 88:1383–1394.
- Taylor KE, Stouffer RJ, Meehl GA (2012) An Overview of CMIP5 and the experiment design. *Bull Am Meteorol Soc* 93:485–498.